JOURNAL OF MATERIALS SCIENCE 29 (1994) 6175–6180

Synthesis of carbon–iron(II) oxide layer on the surface of magnetite and its reactivity with H_2O for hydrogen generation

Y. TAMAURA, K. AKANUMA, N. HASEGAWA, M. TSUJI
Department of Chemistry, Research Center for Carbon Recycling and Utilization, Tokyo Institute of Technology, 2-12-1, Ookayama, Meguro-ku, Tokyo 152, Japan

Synthesis of a carbon–iron(II) oxide layer on the surface of magnetite and its reactivity with H_2O for hydrogen generation reaction have been studied. X-ray diffractometry and chemical analysis showed that the carbon-bearing magnetite synthesized by the carbon-deposition reaction from CO_2 gas with the hydrogen-reduced magnetite, was magnetite with a carbon–iron(II) oxide layer (CIO layer-M; M is stoichiometric magnetite) represented by $(Fe_3O_4)_{1-\delta}(Fe_3O_3)_\delta C_\tau$. The TG-MS spectra also showed the evidence for the formation of the CIO layer on the bulk stoichiometric magnetite. Some amorphous phase was formed in the CIO layer during the activation step (*in vacuo* at 300 °C for 30 min). This amorphous phase reacted with H_2O and evolved H_2 gas at 350 °C. This H_2 generation reaction resulted in the oxidation of the CIO layer into γ-Fe_2O_3 component and the release of a part of carbon in the CIO layer as CO_2. The X-ray diffractometry and Mössbauer spectroscopy indicated that the solid solution of Fe_3O_4–γ-Fe_2O_3 was formed in the solid phase after the H_2 generation reaction. This shows the cation movement in the B site of the bulk magnetite of the activated CIO layer-M during the H_2 generation reaction. The TG-MS spectra also supported the above estimation.

1. Introduction

Magnetite is one of the iron oxides represented by the formula Fe_3O_4 and has a spinel structure. Magnetite is an "inverse" spinel; one-eighth of the tetrahedral sites and one-fourth of the octahedral sites are occupied by trivalent iron ions (Fe^{3+}) while one-fourth of the octahedral sites are occupied by divalent iron ions (Fe^{2+}), and in terms of the spinel structure its formula should be written $Fe^{3+}(Fe^{2+}Fe^{3+})O_4$. Moreover, magnetite has a metal deficit and/or an oxygen excess relative to the stoichiometric composition (Fe_3O_4) and the formula may accordingly be written $Fe_{3-\delta}O_4$ and/or $Fe_3O_{4+\varepsilon}$ in the atmosphere at room temperature [1–5]. On the contrary, although the data for cation-excess and/or oxygen-deficient spinel compounds are very limited, Dieckmann [6] has studied cation-excess magnetite in the temperature range 900–1400 °C, where it exists in equilibrium with wüstite. Recently, Tamaura and Tabata [7] have reported that there exists an oxygen-deficient magnetite around 300 °C, which provided a high reduction activity for stable gaseous oxides such as CO_2 into carbon, in the course of the hydrogen reduction of magnetite into α-Fe. The Mössbauer spectra of the hydrogen-treated magnetite showed only the absorption lines characteristic of the magnetite; two sextet absorption lines appeared. The area ratio of A to B sites increased with an increase in the hydrogen-reduction time (20 min to 120 min), indicating that the Fe^{3+} ions in the B sites are reduced and move into the interstices of the A sites [8]. This shows that the hydrogen-treated magnetite has a deformed spinel structure richer in the A sites number. Thus the hydrogen-treated magnetite is in the oxygen-deficient state with the spinel structure, and is called the oxygen-deficient magnetite. The high reduction reactivity of the oxygen-deficient magnetite for stable gaseous oxides such as CO_2 is closely related to the deformed crystal structure and would be due to the existence of electron hopping in the octahedral sites between Fe^{2+} and Fe^{3+} of the spinel structure. In the CO_2 decomposition reaction, oxygens in CO_2 are incorporated into the solid phase and carbon is deposited on the surface [7–16]. The carbon deposited on the surface exhibits two kinds of carbon with different C–C bond lengths assigned to graphite and amorphous carbon [16]. The iron in the surface layer of the solid phase is not in the form of carbide (Fe_3C) or α-Fe phase, but iron oxide phase. Thus, the surface of the solid phase (carbon-bearing magnetite, CM), formed after the CO_2 decomposition, is considered to be composed of elemental carbon and iron ions.

This paper describes the synthesis of a carbon–iron(II) oxide layer (CIO layer) on the surface of magnetite by repeating the CO_2 decomposition reaction using the hydrogen-reduced magnetite. The hydrogen generation reaction from H_2O with the CIO layer has been studied at 350 °C.

0022–2461

2. Experimental procedure

2.1. Materials

All the chemicals used were of analytical grade, and distilled water was used for the preparation of the solution. $FeSO_4 \cdot 7H_2O$ and NaOH were supplied by Wako Chemical Industries, Ltd. Research-grade hydrogen, carbon dioxide and argon gases were used. Reactant gases used for synthesis of the carbon-bearing magnetite were admitted to the solid reactant in the reaction cell, as will be seen below. Standard gases (hydrogen and carbon dioxide) for calibration were purchased from G. L. Science Co.

2.2. Synthesis of magnetite

Magnetite powder (M) was synthesized by the air oxidation of a hydroxide suspension of Fe(II) according to the wet method reported previously [17–20]. The requisite portion of $FeSO_4 \cdot 7H_2O$ (312 g) was dissolved in oxygen- and CO_2-free distilled water prepared by passing nitrogen gas through for a few hours. The pH of the suspension was adjusted to 10 by adding 3.0 mol dm^{-3} NaOH solution to form a hydroxide suspension. Air was passed through the alkaline suspension for oxidation for 24 h at 65 °C, while the pH was kept constant at 10.

The black precipitate of the synthesized magnetite particles was collected by decantation and washed with distilled water, and acetone successively, and dried in a nitrogen stream at ambient pressure at 50 °C. The X-ray diffraction pattern of the magnetite powder synthesized by the wet method showed a single phase of a spinel-type compound without any other peaks corresponding to α-Fe_2O_3 and iron hydroxides such as α-FeOOH. The lattice constant of the magnetite was 0.8395 nm, which is slightly smaller than that of the stoichiometric magnetite (0.83967 nm) [21]. The chemical composition of the magnetite synthesized was estimated to be $Fe_3O_{4.03}$. These results indicate that the magnetite synthesized by the wet method was slightly oxidized and expressed as the solid solution of $0.91(Fe_3O_4)$–$0.009(\gamma$-$Fe_2O_3)$ for the chemical composition [22, 23].

2.3. Synthesis of the CIO layer-M

After passing hydrogen gas (5.0×10^{-2} dm^3 min^{-1}) through the magnetite powder (3.0 g, 100–200 nm) for 3 h at 300 °C (hydrogen-treatment step), CO_2 gas (5.0×10^{-2} dm^3) was reacted in a quartz cell (1.5×10^{-1} dm^3) for 10 h at 300 °C (carbon-deposition step). We have obtained the carbon-bearing magnetite ($Fe_3O_{4-\delta}C_\tau$; CM) by repeating these two steps three times.

The carbon-bearing magnetite (CM) thus obtained was subjected to X-ray diffractometry with FeK_α radiation (Rigaku, model RAD-2A) to identify the solid phase. The lattice constant of the solid phase was calculated by extrapolating the values of a_0 versus the Nelson–Riley function, to zero, using the least-squares method. The chemical composition of the carbon-bearing magnetite was determined by colorimetry (Hitachi spectrophotometer, model 124) with the 2,2′-bipyridyne for the analysis of the Fe^{2+}/Fe_{total} mole ratio [24], by TG analysis for the oxygen amount using the thermogravimeter (Mac Science, model TG DTA 2000), and by elemental analysis for the carbon amount using an elemental analyser (Perkin–Elmer, model 2400 CHN). X-ray diffractometry and the chemical analysis showed that the carbon-bearing magnetite (CM) thus synthesized was the magnetite with carbon–iron(II) oxide layer (CIO layer-M).

2.4 Synthesis of the CIO layer-M doped with ^{18}O and the magnetite doped with ^{17}O for the TG-MS measurement

The CIO layer-M doped with ^{18}O (CIO layer-M(^{18}O); $Fe_3{}^{18}O_{4-\delta}C_\tau$) was synthesized by the CO_2 decomposition reaction using the $C^{18}O_2$ gas with the oxygen-deficient magnetite (ODM). The stoichiometric magnetite doped with ^{17}O ($Fe_3{}^{17}O_4$) was synthesized by allowing the magnetite powder to stand under a mixed gas atmosphere of $H_2{}^{17}O/H_2$ (1/1000) at 300 °C for 24 h. The CIO layer-M(^{18}O) or the $Fe_3{}^{17}O_4$ was placed in the quartz holder and set up in the electric furnace of the thermogravimeter (Mac Science, model TG DTA 2000). Then hydrogen gas was passed through the sample in the quartz holder to obtain the TG-MS spectra (VG Anatech. Mac Science, model Quadrupoles 560).

2.5. Hydrogen generation reaction using the CIO layer-M

The CIO layer-M (0.2 g) was placed in the reaction cell (diameter 8 mm × 150 mm) and set up in an electric furnace, as shown in Fig. 1. The temperature of the electric furnace, which was measured with a chromel–alumel thermocouple in contact with the outer surface of the reaction cell and controlled to within ±0.3 °C using a regulator (Chino, Model DB1150), was raised to 300 °C, while evacuating the reaction cell using a vacuum pump. After reaching 300 °C, the CIO layer-M was allowed to stand *in vacuo* for 0–60 min at 300 °C (activation step) in the reaction cell. After the activation step, mixed H_2O/Ar gases were flowed through the CIO layer-M at 350 °C. Argon gas passed through the reduced copper to remove the contaminant oxygen at 600 °C. H_2O, which had been bubbled for 30 min by nitrogen to remove dissolved oxygen, was injected into the argon gas stream at the point indicated in Fig. 1, using a syringe. The evolution of gaseous species was determined by mass spectrometry (VG Anatech., model Quadrupoles 560), the excess H_2O was removed from the gas stream by condensation in a glass trap cooled in a refrigerant (NaCl–ice). At the end of the reaction, the reaction cell was quenched in a refrigerant (ice) and the solid phase in the reaction cell was taken out in a nitrogen atmosphere at ambient temperature. The solid phase after the hydrogen-generation reaction was identified by X-ray diffractometry with FeK_α radiation (Rigaku, model RAD-2A) and by Mössbauer spectroscopy with a ^{57}Co source (diffused in metallic rhodium) oscillated in a constant acceleration

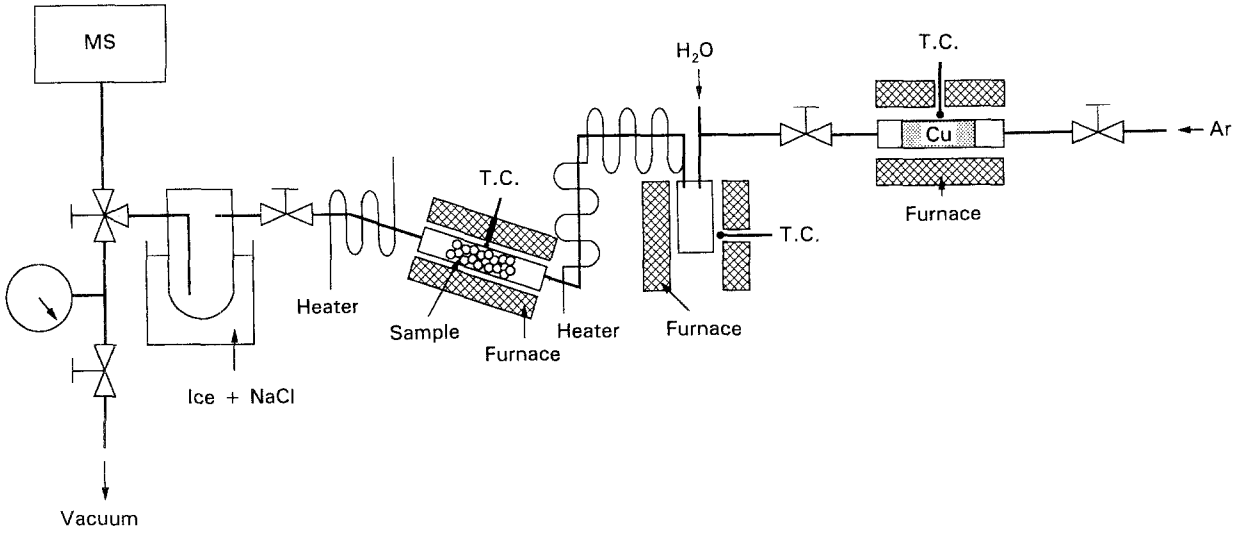

Figure 1 Apparatus for the hydrogen generation reaction.

mode. The Mössbauer spectrum was recorded at room temperature, was calibrated with thin absorbers of an α-Fe foil, and was calculated by a computer-fitting method to pure Lorentzian line shapes. The source was supplied by NEN (UK).

3. Results and discussion

3.1. Synthesis of the CIO layer-M

X-ray diffractometry showed that the CIO layer-M synthesized gave only the peaks of spinel-type structure corresponding to those of magnetite (Fig. 2b), and no peaks corresponding to α-Fe and iron carbide (Fe_3C) appeared. The lattice constant of the spinel-type compound was 0.8397 nm, which is nearly equal to that of the stoichiometric magnetite (0.83967 nm) [21], indicating that the spinel-type compound in the CIO layer-M is the stoichiometric magnetite. The chemical composition of the CIO layer-M was estimated to be $Fe_3O_{4-\delta}C_\tau$ ($\delta = 0.35$, $\tau = 0.17$) from chemical analysis of the iron(II) and (III) contents, the TG analysis of the oxygen amount under flowing hydrogen, and the elemental carbon analysis (Table I). As can be seen from this chemical composition, the total charge of the cations (iron(II) and (III)) and the anion (O^{2-}) is nearly zero, indicating that the CIO layer-M does not contain any metal iron but the iron(II) and (III) ions, even though the δ value is high (0.35). As mentioned above, the lattice constant of the CIO layer-M is nearly equal to that of the stoichiometric magnetite. These findings suggest that the iron in the CIO layer is Fe(II) ion (carbon-iron(II) oxide layer; CIO layer = $(Fe_3O_3)_\delta C_\tau$), and that the bulk (M) of the CIO layer-M is stoichiometric magnetite (M = Fe_3O_4). The CIO layer-M is represented by $(Fe_3O_4)_{1-\delta}(Fe_3O_3)_\delta C_\tau$.

We have further confirmed the formation of the carbon–iron(II) oxide layer (CIO layer) on the bulk magnetite (M = stoichiometric magnetite) from the TG–MS spectra obtained under flowing hydrogen for the CIO layer-M doped with ^{18}O (CIO layer-M(^{18}O); $Fe_3{}^{18}O_{4-\delta}C_\tau$), which had been prepared by the CO_2

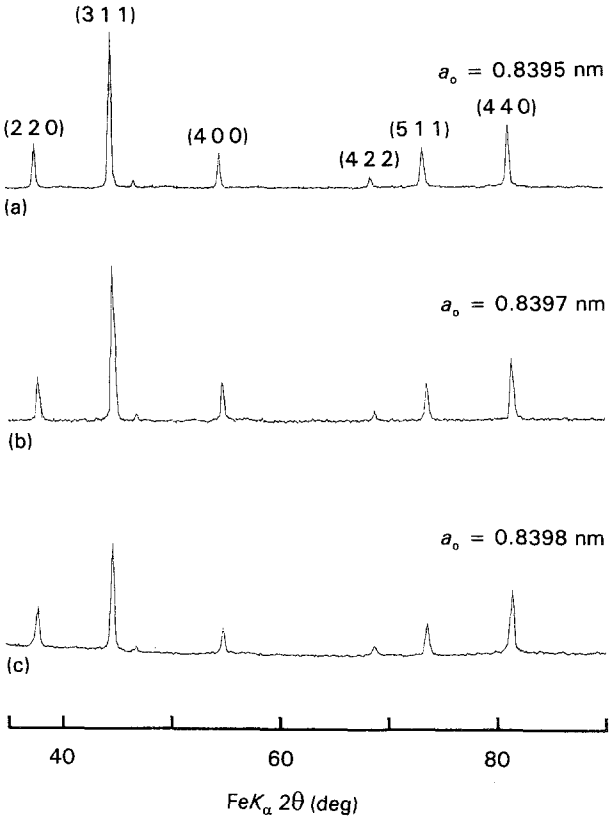

Figure 2 XRD patterns of (a) the magnetite powder synthesized by the air oxidation method ($Fe_3O_{4.03}$), and the CIO layer-M (b) before and (c) after activation by allowing to stand *in vacuo* at 350 °C for 30 min.

TABLE I Chemical composition of the CIO layer-M

	(wt%)	mol/Fe_3O_4
Chemical analysis		
Fe^{2+}	41.2	1.68
Fe^{3+}	32.3	1.32
TG analysis		
O^{2-}	25.6	3.65
Elemental analysis		
C	0.88	0.17

Chemical formula ($Fe_3O_{4-\delta}C_\tau$; $\delta = 0.35$, $\tau = 0.17$).

decomposition reaction using the $C^{18}O_2$ gas. In the TG–MS spectra, the $H_2{}^{18}O$ evolution peak due to hydrogenation of the $^{18}O^{2-}$ ion in the CIO layer-M(^{18}O) appeared around 300 °C ($H_2{}^{18}O$ in Fig. 3b). However, the $H_2{}^{18}O$ evolution was little observed above 400 °C, where the $H_2{}^{16}O$ evolution due to the hydrogenation of the lattice oxygen ($^{16}O^{2-}$) of the bulk (M = stoichiometric magnetite) of the CIO layer-M(^{18}O) ($H_2{}^{16}O$ in Fig. 3b) takes place. For the stoichiometric magnetite doped with ^{17}O ($Fe_3{}^{17}O_4$) by allowing the magnetite powder to stand under a mixed gas atmosphere of $H_2{}^{17}O/H_2$ (1/1000) at 300 °C, the $H_2{}^{17}O$ evolution peak appeared around 450 °C ($H_2{}^{17}O$ in Fig. 3a), which is higher than the $H_2{}^{18}O$ evolution peak of the CIO layer-M(^{18}O) ($H_2{}^{18}O$ in Fig. 3b) by 150 °C. Thus, the $^{18}O^{2-}$ ions localize near the surface of the CIO layer-M(^{18}O). These results suggest that the $^{18}O^{2-}$ ions in the $C^{18}O_2$ are transferred into the oxygen-deficient magnetite in the carbon-deposition step, and that they form the CIO layer(O^{18}) on the surface of the bulk (M) (M = stoichiometric magnetite).

The CIO layer-M thus synthesized is very stable in an air atmosphere and at room temperature, even though the δ value is high (0.35); no changes in the Fe(II)/Fe(III) mole ratio and the lattice constant of the CIO layer-M were observed in an air atmosphere at room temperature for a few days. Thus, the CIO layer-M is not readily oxidized in an air atmosphere, whereas the oxygen-deficient magnetite, $Fe_3O_{4-\delta}$ (δ = 0.1–0.2), which had been prepared by passing hydrogen gas through magnetite at 300 °C, was unstable and reactive towards gases such as oxygen, H_2O and CO_2 and stable only under inert gases such as nitrogen at room temperature. In an air atmosphere, the oxygen-deficient magnetite is gradually oxidized and changes into oxygen-excess magnetite, the iron oxide of the solid solution of Fe_3O_4 and γ-Fe_2O_3, at room temperature.

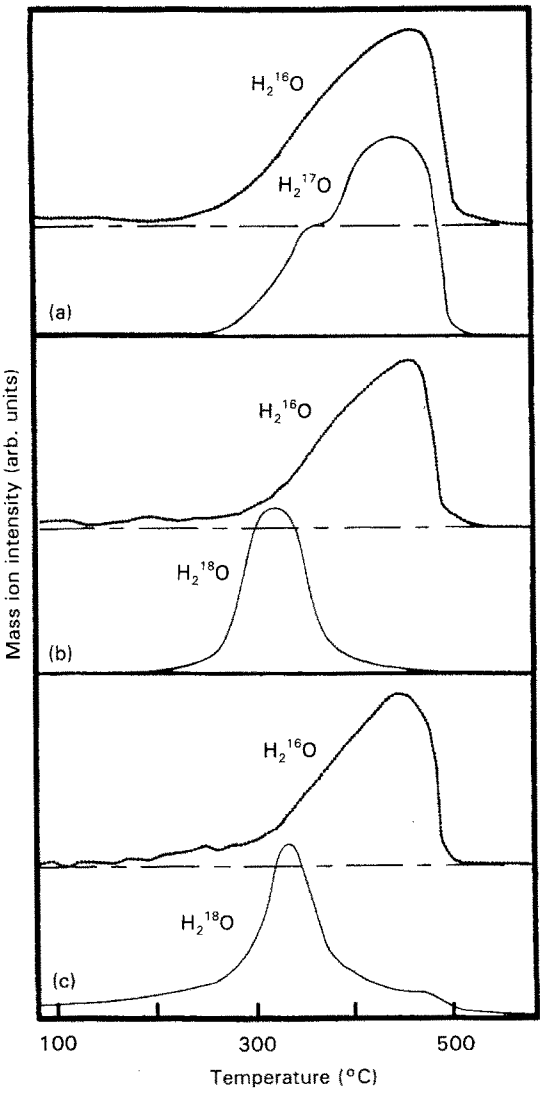

Figure 3 TG-MS spectra taken under flowing hydrogen at 10 °C min^{-1} for (a) the stoichiometric magnetite doped with ^{17}O, and the CIO layer-M doped with ^{18}O (b) before and (c) after the hydrogen generation reaction. The weight decrease in the TG-curves was observed in accordance with the H_2O evolution given by the MS spectra in each panel; therefore, TG curves are omitted and only the MS spectra are given.

3.2. Hydrogen generation from H_2O with CIO layer-M

As described above, the CIO layer-M is stable. However, when the CIO layer-M (0.2 g) was allowed to stand *in vacuo* for 30 min at 300 °C (the activation step), it was found that it became activated (activated CIO layer-M = CIO layer*-M), reacted with H_2O at 350 °C, with the evolution of hydrogen gas (12.5 cm^3 in Table II). The evolved hydrogen gas volume increased with increasing activation time (Table II). After the hydrogen generation reaction, the chemical composition of the CIO layer*-M (after activation for 30 min) was estimated to be $Fe_3O_{4-\delta'}C_{\tau'}$ ($\delta' = -0.12$, $\tau' = 0.071$) from chemical analysis, TG analysis, and elemental carbon analysis. A striking result, that $\delta' < 0$ ($\delta' = -0.12$), was observed, indicating that this hydrogen generation is accompanied by the oxidation of the CIO layer-M into some γ-Fe_2O_3 component. X-ray diffractometry showed that the lattice constant of the CIO layer*-M (after activation for 30 min) after the hydrogen generation reaction (0.8387 nm) was lower than that of the stoichiometric magnetite. Mössbauer spectroscopy showed that some of the iron ions in the B site of the spinel structure were oxidized, compared with stoichiometric magnetite (Fig. 4 and Table III). The X-ray diffractometry and Mössbauer spectroscopy data indicate that a cation vacancy exists characteristic of the B site in the solid solution of Fe_3O_4–γ-Fe_2O_3. Thus, the oxidation of the CIO layer*-M into the γ-Fe_2O_3 component would have resulted in

TABLE II The effect of the activation step for hydrogen evolution from H_2O with CIO layer-M at 350 °C; the activation step means that the CIO layer-M was allowed to stand *in vacuo* at 300 °C

Activation time (min)	H_2 volume (cm^3)
0	6.2
30	12.5
60	13.0

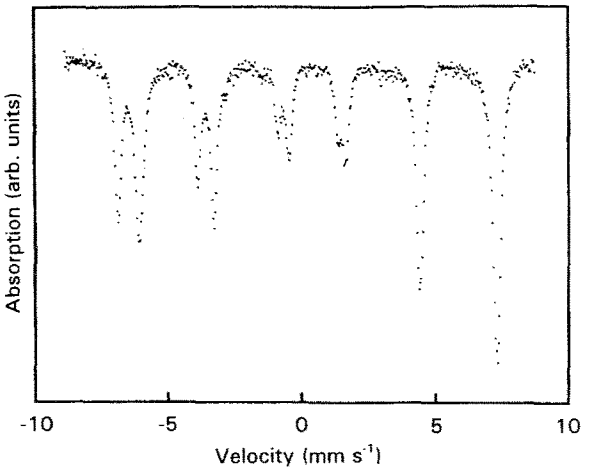

Figure 4 Room-temperature Mössbauer spectrum of the solid solution of $(Fe_3O_4)_{0.76}$ $(\gamma\text{-}Fe_2O_3)_{0.36}$ obtained by hydrogen generation reaction with the CIO layer*-M at 350 °C.

TABLE III Isomer shift and *A/B* area ratio evaluated from the room temperature Mössbauer spectrum of the solid solution of the $(Fe_3O_4)_{0.76}$–$(\gamma\text{-}Fe_2O_3)_{0.36}$ obtained by the hydrogen generation reaction with CIO layer*-M

Isomer shift (mm s^{-1})		*A/B* ratio
A	*B*	
0.29	0.66	0.85

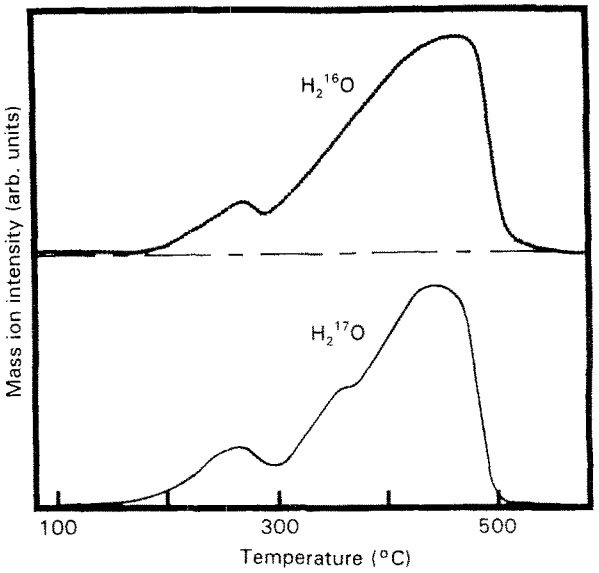

Figure 5 TG–MS spectra taken under flowing hydrogen for 10 °C min^{-1} of the solid solution of $Fe_3O_4(^{17}O)$–$\gamma\text{-}Fe_2O_3(^{17}O)$.

cation movement in the B site of the bulk magnetite (M), and generated a cation vacancy. This would have eventually resulted in the formation of the solid solution of Fe_3O_4–$\gamma\text{-}Fe_2O_3$. The chemical composition of the solid solution obtained after the hydrogen generation reaction with CIO layer*-M (after activation for 30 min) was estimated to be $(Fe_3O_4)_{0.76}(Fe_2O_3)_{0.36}$ from chemical analysis and the Mössbauer spectrum. In the TG–MS spectra taken under flowing hydrogen

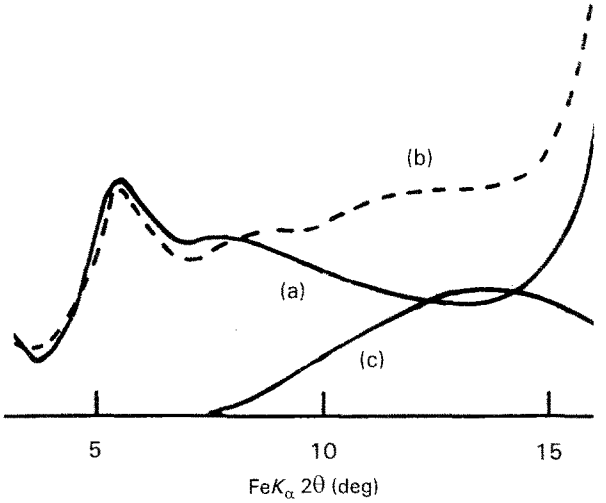

Figure 6 XRD patterns of the CIO layer-M (a) before and (b) after activation by allowing to stand *in vacuo* at 350 °C for 30 min. (c) The X-ray turbidity measured from the XRD intensity difference between (a) and (b).

for the solid phase obtained after the hydrogen generation reaction using the CIO layer-M(^{18}O), a broadened $H_2{}^{18}O$ evolution peak ($H_2{}^{18}O$ in Fig. 3c) appeared around 150–250 °C. This broadening is due to the hydrogenation of the $^{18}O^{2-}$ ion in the $\gamma\text{-}Fe_2O_3$ component around 150–250 °C; a solid solution of $Fe_3O_4(^{17}O)$–$\gamma\text{-}Fe_2O_3(^{17}O)$ gives a similar broadened peak ($H_2{}^{17}O$ in Fig. 5) around 150–250 °C. These results also support that the $\gamma\text{-}Fe_2O_3$ component is formed in the hydrogen generation reaction.

Because the hydrogen generation presented here requires an activation step, as mentioned above, it is considered that some reactive phase is formed in the CIO layer during the activation step; the CIO layer changes into some activated form (CIO layer*-M). In the X-ray diffraction pattern of the CIO layer*-M (after activation for 30 min), neither peaks of metal iron nor those of carbides appeared, and only a lowering of the peak intensity of the spinel-type compound was observed (Fig. 2c). The lattice constant of the spinel-type compound was 0.8398 nm, which is nearly equal to that of the unactivated CIO layer-M. Moreover, as can be seen from Fig. 6, a distinct enhancement in the X-ray turbidity was observed in the lower diffraction angle region around $2\theta(Fe K_\alpha) = 10°–15°$. This indicates that some amorphous phase was formed in the CIO layer*-M.

During the hydrogen generation reaction from H_2O with the CIO layer*-M at 350 °C, the CO_2 gas (1.9×10^{-3} dm^3) was also evolved whose volume is about 15% of that of hydrogen gas ($H_2/CO_2 = 6.7/1.0$). The carbon content in the CIO layer-M decreased from $\tau = 0.17$ to 0.071 during the hydrogen generation reaction. These results indicate that the carbon in the CIO layer was released as CO_2 gas.

It is considered that the amorphous phase in the CIO layer*-M is transformed into the $\gamma\text{-}Fe_2O_3$ component in the hydrogen generation reaction. Because CIO layer is piled up on the bulk magnetite (M) with the spinel structure, the spinel structure of the bulk magnetite would make it easy for the iron ions and

oxygen ions in the CIO layer to form the spinel structure during the oxidation of the iron(II) ions in the CIO layer with H_2O.

Acknowledgements

This work was partially supported by a Grant-in-Aid for Science Research 03203216 from the Ministry of Education, Science and Culture. One of the authors (K. Akanuma) is grateful for grants from fellowships of the Japan Society for the Promotion of Science for Japanese Junior Scientists.

References

1. L. S. DARKEN and R. W. GURRY, *J. Am. Chem. Soc.* **67** (1945) 1398.
2. *Idem, ibid.* **68** (1946) 798.
3. J. SMILTENS, *ibid.* **79** (1957) 4877.
4. *Idem, ibid.* **79** (1957) 4881.
5. O. N. SALMON, *J. Phys. Chem.* **65** (1961) 550.
6. R. DIECKMANN, *Ber. Bunsenges. Phys. Chem.* **86** (1982) 112.
7. Y. TAMAURA and M. TABATA, *Nature (Lond.)* **346** (1990) 255.
8. Y. TAMAURA, in "Proceedings of the International Symposium on Chemical Fixation of Carbon Dioxide", Nagoya, December 1991, edited by K. Ito (The Chemical Society of Japan, 1991) p. 167.
9. K. NISHIZAWA, T. KODAMA, M. TABATA, T. YOSHIDA, M. TSUJI and Y. TAMAURA, *J. Chem. Soc. Faraday Trans.* **88** (1992) 2771.
10. K. AKANUMA, K. NISHIZAWA, T. KODAMA, M. TABATA, K. MIMORI, T. YOSHIDA, M. TSUJI and Y. TAMAURA, *J. Mater. Sci* **28** (1993) 860.
11. Y. TAMAURA, in "Proceedings of the Sixth International Conference on Ferrites" (ICF 6), Tokyo and Kyoto, September 1992, edited by T. Yamaguchi and M. Abe (The Japan Society of Powder and Powder Metallurgy, 1992) p. 195.
12. K. AKANUMA, K. NISHIZAWA, T. KODAMA, M. TABATA, T. YOSHIDA and Y. TAMAURA, *ibid.*, p. 229.
13. K. NISHIZAWA, T. KODAMA, M. TABATA, T. YOSHIDA and Y. TAMAURA, *ibid.* p. 239.
14. M. TABATA, T. KODAMA, K. AKANUMA, K. NISHIZAWA, T. YOSHIDA and Y. TAMAURA, *ibid.*, p. 246.
15. M. TABATA, Y. NISHIDA, T. KODAMA, K. MIMORI, T. YOSHIDA and Y. TAMAURA, *J. Mater. Sci.* **28** (1993) 971.
16. K. AKANUMA, M. TABATA, N. HASEGAWA, M. TSUJI, Y. TAMAURA, Y. NAKAHARA and S. HOSHINO, *J. Mater. Chem.* **3** (1993) 943.
17. Y. TAMAURA, S. MECHAIMONCHIT and T. KATSURA, *J. Inorg. Nucl. Chem.* **43** (1980) 671.
18. T. KATSURA, Y. TAMAURA and G. S. CHYO, *Bull. Chem. Soc. Jpn* **52** (1979) 96.
19. Y. TAMAURA, P. V. BUDUAN and T. KATSURA, *J. Chem. Soc. Dalton Trans.* (1981) 1807.
20. M. KIYAMA, *Bull. Chem. Soc. Jpn* **47** (1974) 1646.
21. JCPDS cards 19-629 (Joint Committee on Powder Diffraction Standards, Swarthmore, PA, 1989).
22. Y. TAMAURA, T. KODAMA and T. ITOH, *J. Am. Ceram. Soc.* **73** (1990) 3539.
23. K. KODAMA, *J. Mater. Chem.* **2** (1992) 525.
24. I. IWASAKI, T. KATSURA, T. OZAWA, M. YOSHIDA, M. MASHIMA, H. HARAMURA and B. IWASAKI, *Bull. Volcanol. Soc. Jpn Ser. II* **5** (1960) 9.

Received 12 October 1993
and accepted 16 May 1994